Health Monitoring of Aligned Carbon Nanotube (CNT) Enhanced Composites

Derreck M. Barber, Sunny S. Wicks, Brian L. Wardle[1]
Technology Laboratory for Advanced Materials and Structures (TELAMS)
Dept. of Aeronautics and Astronautics
Massachusetts Institute of Technology
77 Massachusetts Ave.
Cambridge MA 02139

Ajay Raghavan, Christopher T. Dunn, and Seth S. Kessler
Metis Design Corporation
10 Canal Park
Cambridge MA 02141

ABSTRACT

Hybrid advanced composites, termed nano-engineered composites, have been developed that are comprised of aligned carbon nanotubes (CNTs), epoxy resin, and advanced fibers. While the CNTs occupy ~1% of the volume of these bulk nanostructured composites, due to alignment and distribution, significant strength and toughness enhancement has been observed (*e.g.,* more than 100% increase in interlaminar fracture toughness). A multifunctional aspect of these materials is electrical conductivity that is enhanced by many orders of magnitude (10^6 and 10^8, in-plane and through thickness, respectively). This multifunctional aspect is utilized to solve challenges in a resistive structural health monitoring (SHM) sensing concept. Composites present significant challenges for inspection due to their heterogeneity and anisotropy, the fact they fail by interacting modes, and since damage often occurs beneath their surface. Current effective laboratory non-destructive methods, such as X-ray and C-scan, are impractical for inspection of large integrated structures. Resistive SHM methods have been investigated previously, however they are hindered by small measurements (high resistivity giving rise to high noise-to-signal) and interconnection issues. Both issues may be addressed by the increased conductivity in the nano-engineered composites and by creating electrical break-out connections through 3-D leads brought to the surface. Undamaged and damaged 2-ply 'fuzzy-fiber' composites are inspected using a simple surface-mounted electrode configuration, and sensitivity to damage (both in-plane and through-thickness) is demonstrated. Future work includes improvements in sensor-structure integration and evaluation of strength-after-impact via impact and subsequent tensile testing.

1. INTRODUCTION

Composite materials are increasingly replacing metals in the aerospace industry. These advanced composites offer weight-saving improvements such as high specific strength and stiffness while providing resistance to fatigue and corrosion. These systems are not without disadvantages, however. Traditional advanced composites exhibit significantly reduced electrical and thermal conductivity relative to metals, and matrix-rich regions at ply interfaces results in relatively poor

[1] wardle@mit.edu, (617) 252-1539

interlaminar properties. Additionally, composites that have sustained damage often have non-visible or barely-visible damage, complicating damage assessment. Recent efforts to address the limitations of advanced composites include the incorporation of carbon nanotubes (CNTs) into the polymer matrix of the composite. Exceptional physical properties of CNTs including mechanical stiffness (as high as 1 TPa in some experiments) and electrical conductivity (~1000x copper under certain conditions) make them an attractive constituent in traditional composites. Capturing these nanoscale properties in a macroscale material presents many challenges: issues with dispersion, alignment and feasible volume fraction of the CNTs limits bulk property improvements. The work presented in this paper proposes strategically placing aligned CNTs to overcome scaling issues and address mechanical limitations seen with traditional composites, and to assess the feasibility of using enhanced electrical conductivity in a structural health monitoring concept.

Nano-engineered composites allow control of the location and direction of CNTs to optimize reinforcement directions. Here, CNTs are arranged radially on the surfaces of advanced and infiltrated with epoxy to create 'fuzzy-fiber' reinforced plastics (FFRP) [1, 2], as shown in Figure 1. The use of CNTs serves a multi-faceted purpose: while reinforcing matrix regions between fibers and between plies is the primary objective, secondarily, percolating conductive networks are created that vastly improve conductivity of the bulk composite material. Past work indicates a significant (10^6 – 10^8) increase of electrical conductivity of the FFRP, as shown in Figure 2 as a function of CNT volume fraction. Such enhanced conductivity enables advanced structural health monitoring techniques that may detect internal damage before it can be visually identified.

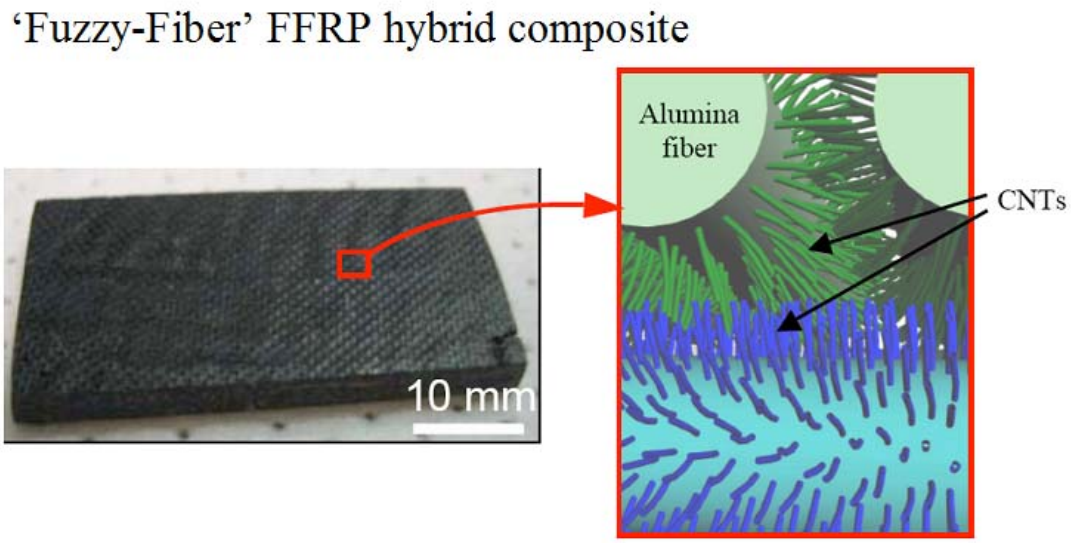

Figure 1. Laminate composed of cloth containing fibers (in tow form) with *in situ*-grown aligned CNTs in a polymer matrix (left), and illustration of cross-sectional region between tows (right). CNTs grown on the surface of each fiber interact with CNTs of nearby fibers achieving inter-tow and interlaminar reinforcement [3].

Structural health monitoring (SHM) has been established as a route to assess the level of damage in a composite without relying on visual inspection. CNT-enhanced composites show promise to improve the conductivity of composites allowing for monitoring systems that can measure changes in resistance in real time to discover local damage before catastrophic failure [5, 6]. Thostenson and Chou built CNT-enhanced advanced fiber-reinforced composites with improvements in electrical conductivity and had encouraging results in damage monitoring using passive in-plane electrical resistance measurements [7]. However, their approach to incorporating CNTs in the fiber-reinforced composite results in random alignment of short and very low volume fraction CNTs, resulting in no significant improvement in mechanical properties. Further, their coupon-level approach to SHM used *in-plane* resistance measurements that would require a dense network of invasive wiring and instrumentation for practical large-area monitoring. Thus, a novel approach to incorporating CNTs in fiber-reinforced aerospace structural composites for SHM is implemented here, whereby all the potential advantages of CNTs are used for improving mechanical properties as well as enabling SHM with a less invasive electrode network.

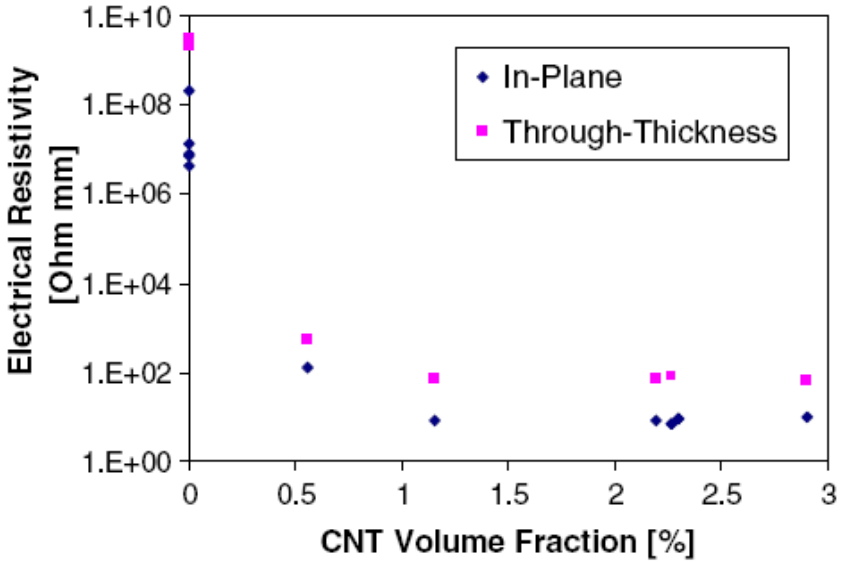

Figure 2. Electrical resistivity of FFRP for in-plane and through-thickness directions vs. CNT volume fraction [4].

2. EXPERIMENTATION

In this section, the synthesis of CNTs and the manufacturing process of baseline (no CNTs) and FFRP (with CNTs) laminates are described, as well as sensor testing protocols.

2.1 Sample Manufacturing

Composite samples are fabricated using a woven alumina ceramic cloth. Aligned CNTs are grown using a process called chemical vapor deposition (CVD) [8]. As-manufactured alumina cloth is dipped in a 50mM solution of isopropanol and iron nitrate, coating individual fibers with the iron catalyst including those inside every tow. The dip-coated cloth is dried in ambient air

then placed in a thermal CVD tube furnace. The system is heated in a hydrogen environment that reduces the catalyst on the surface of the fibers into small iron particles. Ethylene gas is then introduced, which decomposes and reacts with the catalyst particle to grow aligned nanotube forests. The CNTs extend perpendicular to the fiber surface and bridge neighboring fibers and plies [9], as depicted in Figure 1. The CNTs are typically longer than the spacing between the composite plies (~10 μm) and between the fibers (~ 1-5μm). A fuzzy-fiber ply and laminate are shown in Fig. 3.

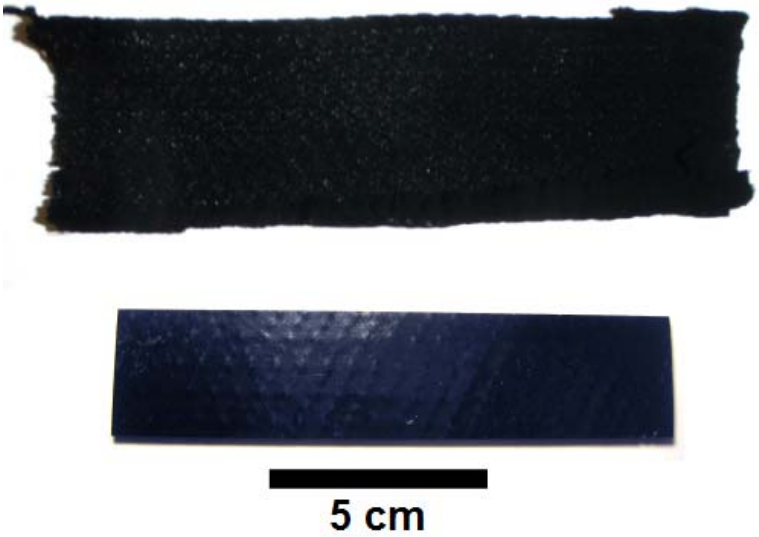

Figure 3. A fuzzy fiber ply (top) and FFRP laminate (bottom).

Both the baseline and FFRP specimens were manufactured to be two plies thick using hand lay-up, following the procedure illustrated in Figure 4. Each cloth layer is placed on a sheet of non-porous Teflon (GNPT) and coated in West Systems epoxy (Resin 105 and Hardener 206). The epoxy is wicked into the interior of the woven ply within a few seconds, after which another ply is placed on top. The aligned CNT forests assist with wetting the ply, as it has been shown that aligned forests wet easily and draw epoxy into the forest by capillary action [4, 10]. After the laminate is created, porous Teflon (PT), absorbent bleeder paper, and GNPT are placed over the laminate. A caul plate and vacuum are then used to provide pressure to the assembly and ensure uniform thickness. After curing for at least 12 hours, the sample is wet-trimmed with a diamond-grit cutting wheel.

2.2 Experimental Testing

Experimental tests to study the enhancement of structural health monitoring with an increase in laminate conductivity are studied using previously developed SHM procedures. A non-invasive silver-ink electrode grid and multiplexing micro-switches will be connected to compact hardware for through-thickness resistance measurements in the full implementation. The painted electrode grid, inspired by flat panel liquid crystal display (LCD) technology, uses an “active” layer of electrode columns on one surface of the laminate as a positive electrode, and on the other surface another layer of electrode rows will act as “passive” ground (see Figure 5). By cycling through particular row and column selections, local through-thickness resistance measurements can be obtained for a grid of points over the structure, in addition to in-plane data.

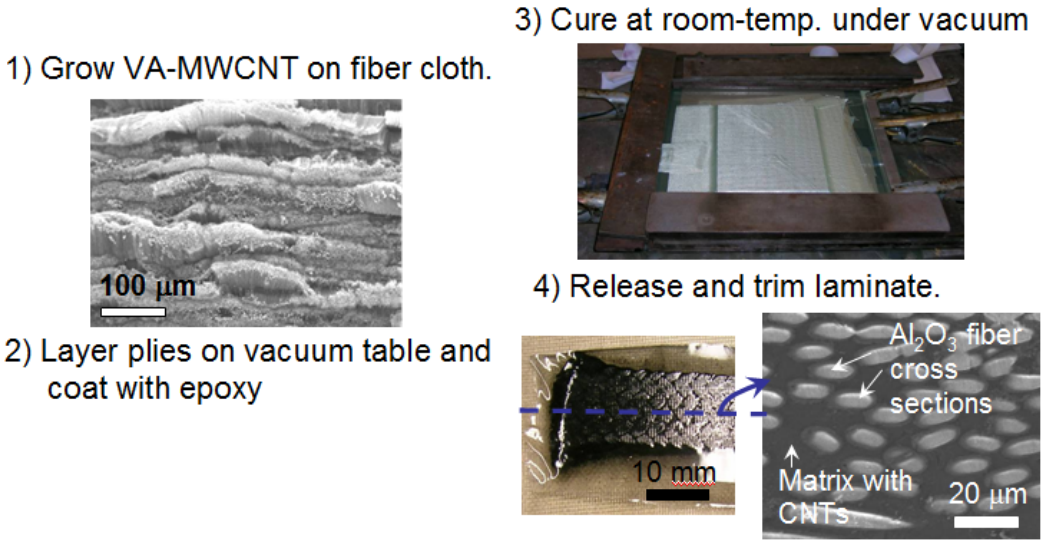

Figure 4. Hand lay-up procedure used to fabricate all laminates in this work.

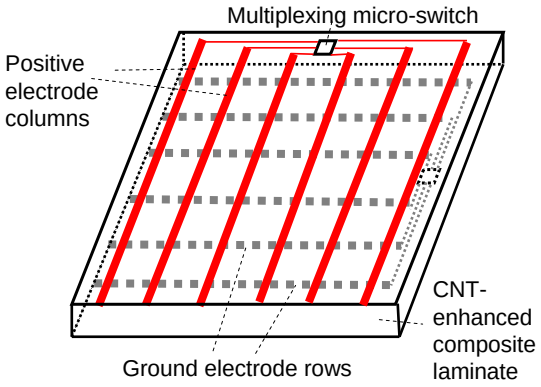

Figure 5. Proposed non-invasive silver ink electrode and multiplexing switch for through-thickness and in-plane conductivity measurements of a composite laminate.

Structural damage in the form of delamination and cracks affect local through-thickness (and in-plane) resistance, especially for CNT-enhanced specimens where a percolating CNT network is created. By interpolating between measurements at distinct grid points with the electrode network, high-resolution through-thickness electrical-resistance-change maps over large structural areas can be obtained, allowing for accurate localization of damage. Using through-thickness resistance from non-invasive techniques as the monitoring parameter allows for easy scaling with low mass and space penalty, which is crucial in aerospace structures. Because secondary considerations such as static mechanical load and hysteresis effects affect resistance measurements, results must be carefully examined to distinguish damage from these factors [11].

Two specimen groups were fabricated: baseline and FFRP specimens. A complete test matrix of 3 baseline and 8 FFRP specimens is planned, however to date 4 specimens have been

manufactured using this technique: 2 with fuzzy fiber plies and 2 with plain alumina (baseline laminate). The two baseline laminates have dimensions of 4.5 x 1 x 0.08 in (114 x 25 x 2 mm), while the two FFRP samples have dimensions of 4.5 x 1 x 0.12 in (114 x 25 x 3 mm). On the top surface, 22 parallel conductors were patterned in the short-dimension, and 4 parallel conductors were patterned in the long dimension on the opposite surface as shown in Figs. 6 and 7.

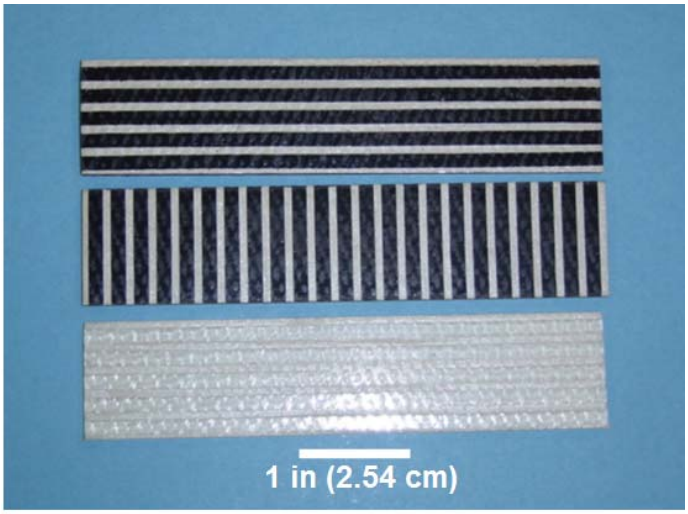

Figure 6. Two FFRP samples and one baseline sample with silver paint stripe electrodes.

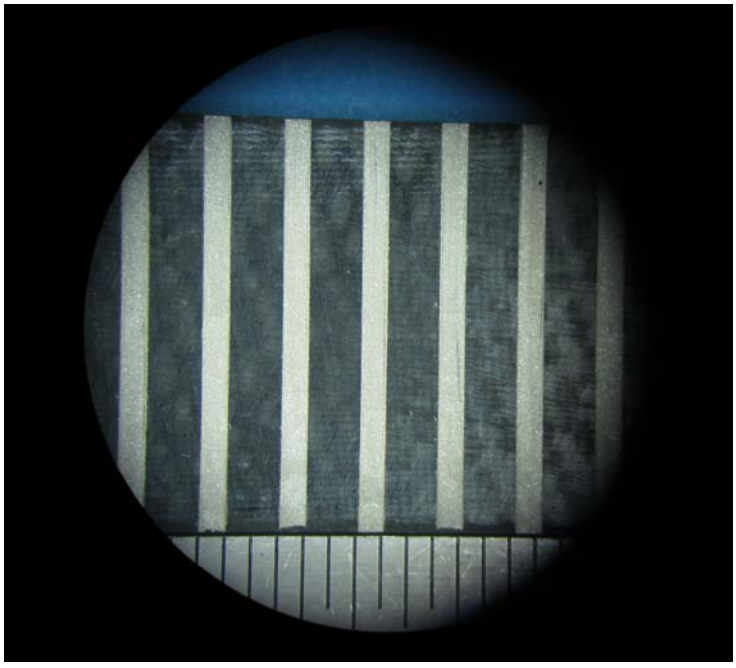

Figure 7. Close-up image of an electroded FFRP laminate. Each tick mark along the bottom is 1.6 mm (1/16").

Prior to impact, the resistance of each specimen was measured: 1) between each parallel trace in-plane, and 2) at each grid point created by the intersection of perpendicular top and bottom traces through-thickness. Initial data showed significant variability when probing directly on the silver traces. To address this issue, a procedure was developed that involved bonding thick gauge wire to the traces using silver epoxy, resulting in < 2% change across 10 repeat trials. Each of the specimens (1 baseline and 1 FFRP to date) was impacted with 75 ft-lbs using a guided dropped weight impact device, calibrated to cause minor surface micro-cracking on the composite surface. Following impact, post-damage electrical resistance measurements were collected again for each possible combination. Photographs of each specimen were also taken before and after impact under microscope in order to document the effects of the impact event on the surface of each specimen.

3. RESULTS

Following impact, no damage was visible to the unaided eye for either specimen. Microscopy however revealed cracking on the back surface (opposite from the impact surface) of both the baseline and FFRP laminates, as seen in Figure 3 for the FFRP specimen. The original planned experiment had called for an analog multiplexer to switch electrode pairs for ease of measurement, however, due to time constrains the previously described instrumentation process was implemented for the presented results. Two sets of data were collected for the pre- and post-impact damage evaluation: 1) in-plane between each parallel pair of adjacent traces, and 2) through-thickness at each grid point created by the virtual intersection of the perpendicular top and bottom surface traces.

First, for the baseline laminate, all measured values for both in-plane pairs and through-thickness pairs were higher than the range of the multimeter (5 MΩ) before and after impact. It was clearly evident that without the CNT enhancements, there is no suitable conductive path formed for electrical evaluation. Next, data was collected for the in-plane resistance of the FFRP. For the short traces the average resistance is 9 Ω pre-impact. Following impact, while the outermost trace pairs on either side of the damage site along the x-axis showed < 10% change, the middle was consistently > 100%. Only minor changes (< 1%) were detected between long trace pairs. Finally, electrical resistance data was collected for the 56 through-thickness grid points, which averaged 20 Ω pre-impact. As seen in Figure 8, a clear change of > 100% was detected in the impacted region. Along the x-axis, between the measurement points for the long traces (left edge in Figure 8) and the damage site, < 10% change was observed. However on the opposite side of the damage site (right side of Figure 8), a constant resistance offset was introduced due to the presence of cracks across the backface electrodes.

It is interesting to note that the result do not show peak changes exactly at the center of the impact target. This may indicate that the parameters are sensitive to different damage modes. For instance, in-plane resistance may be more sensitive to surface cracks, which tend to form at the edge of the impact zone. Conversely, through-thickness resistance may be more sensitive to delamination, which would affect the CNT links across the specimen plies.

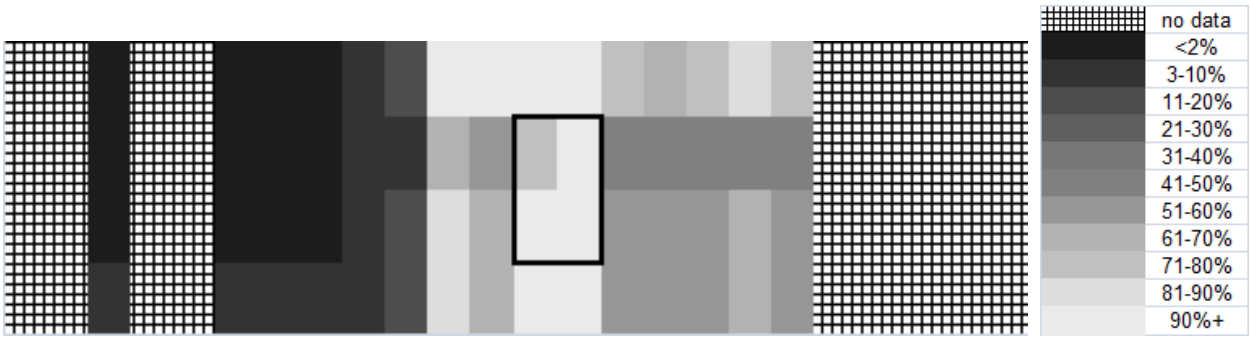

Figure 8. Representation of the through-thickness resistance change after impact. Hashed regions denote where no data was taken. The square box in the center indicates the approximate impact location.

4. CONCLUSIONS

CNT-enhanced composites were fabricated, patterned with a silver ink electrode grid, and subsequently subjected to impact damage. Both in-plane and through-thickness electrical resistance measurements were collected. Clear changes were observed in both sets of data for traces close to the impacted zone of the specimen, demonstrating that these parameters were sensitive to damage in the structure. The peak changes were close to the center of the specimen near the impact site, and there was little to no change in values at points away from the damage zone. Overall, the barely visible impact damage caused significant resistance change, which will allow for a full-field representation of the damage locations by interpolating the collected data. This demonstrates the potential of using this approach as an SHM solution, with the added benefit of CNTs reinforcing the structure.

Near-term research will aim to further validate this method with additional specimens in a more comprehensive test matrix, as well as to observe the effects of multiple progressive impact events. Furthermore, pre- and post-damage tensile tests will be conducted to evaluate residual strength and stiffness for baseline and FFRP laminates. Future work will implement the multiplexed circuit originally envisioned and leverage direct-write technology to create more accurate electrode grid formations.

5. ACKNOWLEDGMENTS

This research was sponsored by the Air Force Office of Scientific Research (AFOSR) under the Phase I STTR contract FA9550-09-C-0165. The work was performed at the Metis Design Corporation in Cambridge, MA and at MIT's Department of Aeronautics and Astronautics, in Cambridge, MA. Derreck Barber gratefully acknowledges support from the Paul E. Gray (1954) Endowed Fund for UROP.

6. REFERENCES

1. Garcia, E.J., Hart, A.J., Wardle, B.L., and Slocum, A. *Fabrication and Testing of Long Carbon Nanotubes Grown on the Surface of Fibers for Hybrid Composites*. in *47th AIAA/ASME/ASCE/AJS/ASC Structures, Structural Dynamics, and Materials Conference*. 2006. Newport, R.I.
2. Garcia, E.J., J.A. Hart, and B.L. Wardle, *Long Carbon Nanotubes Grown on the Surface of Fibers for Hybrid Composites.* AIAA Journal, 2008. **46**(6): p. pp.1405-1412.
3. Wardle, B.L., Bello, D., Ahn, K., Yamamoto, N., Guzman deVilloria, R., Hallock, M., Garcia, E.J., and A. John Hart. *Particle and Fiber Exposures During Processing of Hybrid Carbon-Nanotube Advanced Composites*. in *2008 SAMPE Fall Technical Conference*. Sep. 2008. Memphis, TN.
4. Garcia, E.J., et al., *Fabrication and Multifunctional Properties of a Hybrid Laminate with Aligned Carbon Nanotubes Grown In Situ.* Composites Science and Technology, 2008. **68**(9): p. 2034-2041.
5. Thostenson, E.T. and T.-W. Chou, *Real-time in situ sensing of damage evolution in advanced fiber composites using carbon nanotube networks.* Nanotechnology, 2008. **19**(21): p. 215713.
6. Li, C., E.T. Thostenson, and T.-W. Chou, *Sensors and actuators based on carbon nanotubes and their composites: A review.* Composites Science and Technology, 2008. **68**(6): p. 1227-1249.
7. Thostenson, E.T., Chou, T.-W.,, *Carbon Nanotube Networks: Sensing of Distributed Strain and Damage for Life Prediction and Self Healing.* Advanced Materials, 2006. **18**(21): p. 2837-2841.
8. Yamamoto, N., et al., *High-yield growth and morphology control of aligned carbon nanotubes on ceramic fibers for multifunctional enhancementof structural composites.* Carbon, 2008.
9. Wicks, S.S., et al. *Interlaminar Fracture Toughness of a Woven Advanced Composite Reinforced with Aligned Carbon Nanotubes*. in *50th AIAA/ASME/ASCE/AHS/ASC Structures, Structural Dynamics, and Materials Conference*. 2009. Palm Springs, CA.
10. Garcia, E.J., et al., *Fabrication of composite microstructures by capillarity-driven wetting of aligned carbon nanotubes with polymers.* Nanotechnology, 2007. **18**(16): p. 165602.
11. E. T. Thostenson, T.-W.Chou, *Carbon Nanotube Networks: Sensing of Distributed Strain and Damage for Life Prediction and Self Healing.* Advanced Materials, 2006. **18**(21): p. 2837-2841.